24th COBEM - 2017

24th ABCM International Congress of Mechanical Engineering
December 3-8, 2017, Curitiba, PR, Brazil

COBEM-2017-0531
SHAPE DISTORTIONS OF ANGLED SANDWICH STRUCTURES

Olumide Mayowa Makinde
Mechanical Engineering Division Technological Institute of Aeronautics-ITA
olumidemakinde@yahoo.com
Alfredo Rocha de Faria
Mechanical Engineering Division Technological Institute of Aeronautics-ITA
arfaria@ita.br
Mauricio Vicente Donadon
Aerospace Engineering Division Technological Institute of Aeronautics-ITA
donadon@ita.br

Abstract. *Shape distortions are a major source of problems for composite manufacturers. Moreso, these shape distortions are more emphasized in sandwich panels due to their inherent strengths and improved resistance to bending. In this paper, the analytical model developed by Fernlund for angled sandwich panels was extended to capture cure shrinkage effect. The results of the analytical model enables the evaluation of the contributions of the thermal and cure shrinkage effect to the spring-in phenomenon. Additionally, the results of the analytical model was then compared with Svanberg model implemented using UMAT in Abaqus. The results of both models show good accuracy in their prediction of Spring-in behaviours of Angled Composite Sandwich panels. The analytical model shows that the thermal contribution of the sandwich panels remain fairly constant irrespective of the percentage content of the sandwich core while the contributions of the shrinkage effect reduces.*

Keywords:*Residual stresses, Shape distortions, Spring-in, Sandwich panels, Composite*

1. INTRODUCTION

Shape distortions of composite structures can be a major source of problems in the manufacturing of composite structures. These distortions; which are process induced; makes the manufacturing of composite parts an iterative and expensive process, involving the modification of tool profiles after initial trials to compensate for distortions (Mahadik and Potter, 2013). Distortions and residual stresses are inherently present in advanced composite structures that undergo curing cycles at elevated temperature. Residual stresses are the driving mechanisms to induced distortions but they also have the potential to significantly and adversely reduce the strength of composite structures (Faria, 2015).

There are several phenomena that can cause process-induced deformations and lead to poor dimensional control. These include resin bleed, tool expansion, mechanical tool-part interaction, cure gradients, and anisotropic shrinkage (Pagliuso, 1982; Ridgard, 1993). While it is difficult to completely avoid process-induced deformations, the most common strategy employed in industry is to compensate the manufacturing tool for the anticipated deformation. However, this approach is often not successful. This is because the process-induced deformations is generally unknown until the tool is cut and the part is made. Attempts to transfer measured deformations from a prototype part is not always successful as the process-induced deformations to some extent are dependent on the cure history of the part, which in turn is dependent on the process tool (Fernlund, 2005).

In the aerospace and wind turbine industry, sandwich constructions are often used due to their high stiffness to weight ratio in addition to their resistance to bending. However, angled sandwich panels can experience distortions; commonly referred to as spring-in effect; and the resulting problem is often greater than that experienced by solid laminates due to their high stiffness (Fernlund, 2005). The core contributes significantly to the thermal response of the structure. However, it does not contribute to the chemical shrinkage and frozen in strains. The study seeks to evaluate the contributions of sandwich core to the spring-in effect.

2. BACKGROUND

There have been similar works in the area of shape distortions of composite structures. Similarly, several models exist for the prediction of shape distortions(Stephan et al., 1996; Wang et al., 1992; Johnston et al., 1996; Kim and White, 1997; Wiersma et al., 1998a). In Fig. 1, Radford and Rennick (1997) showed that the spring-in angle, for corner sections can be

predicted from geometry and expansion strains by using Eq. (1).

$$\Delta\theta = \theta\left[\frac{\varepsilon_1 - \varepsilon_3}{1+\varepsilon_3}\right] \approx \theta(\varepsilon_1 - \varepsilon_3) \tag{1}$$

where ε_1 and ε_3 are the free expansion in the in-plane and through-thickness directions respectively. $\Delta\theta$ is the spring-in angle and θ is the angle surrounded by the bend. Equation (1) can be modified to capture the contributions of thermal expansion and cure shrinkage as described in Eq. (2).

$$\Delta\theta = \theta * \left[\frac{(\alpha_1 - \alpha_3)\Delta T}{1+\alpha_3\Delta T} + \frac{\beta_1 - \beta_3}{1+\beta_3}\right] \tag{2}$$

Where ΔT is the change in temperature, α_1 and α_3 are the coefficient of thermal expansion in the in-plane and transverse directions respectively. In addition, β_1 and β_3 are the coefficient of chemical shrinkage in the in-plane and transverse directions respectively. Equation (2) effectively says that the total spring-in is a contribution of spring-in from thermal expansion/contraction and spring-in from cure shrinkage.

$$\Delta\theta = \Delta\theta_{th} + \Delta\theta_{shrinkage} \tag{3}$$

While Eq. (3) can be used to predict spring-in of angled shaped components, it does not capture the effect of other contributors such as frozen in strains, tool part interaction, cure schedule among others. However, the contributions of chemical shrinkage and thermal effect present the largest contributions to the spring-in phenomenon with Wiersma et al. (1998b) stating that the thermal contribution to spring-in is almost 67% percent of the overall value. To capture the effect of the contributions of the sandwich core to the spring-in phenomenon, Fernlund (2005) presented a simple analytical model for the prediction of thermo-elastic spring-in of angled composite sandwich panels as shown in Eq. (4).

$$\Delta\theta = \left\{\theta_0 * \left(\frac{1+\varepsilon_{\phi s}}{1+\varepsilon_{rs}}\right) * \left(\frac{1}{1+\frac{\varepsilon_{rc}-\varepsilon_{rs}}{(1+{}^{t_0}/_{c_0})(1+\varepsilon_{rs})}}\right)\right\} \tag{4}$$

Where θ_0 represents the initial angle of the structure, ε_{rc} is the radial strain of the core and ε_{rs} is the radial strain of the skin. In addition, $\varepsilon_{\phi s}$ is the tangential strain of the skin while t_0 and c_0 are the initial thickness of the skin and initial core thickness respectively. Fernlund concluded that the effect of the core on spring-in is a function of the difference between the through the thickness strains of the core and the skins. If the thermal radial strain of the core was more than that of the skin, then the spring-in would increase and vice versa. The model by Fernlund (2005) only considered thermal effects of the core and ignored effects of resin cure shrinkage. In order to capture the effects of cure shrinkage, Eq. (4) can be modified in accordance with Eq. (3) to obtain Eq. (5)

$$\Delta\theta = \theta_0 * \left[\left\{\left(\frac{1+\varepsilon_{\phi s}}{1+\varepsilon_{rs}}\right) * \left(\frac{1}{1+\frac{\varepsilon_{rc}-\varepsilon_{rs}}{(1+{}^{t_0}/_{c_0})(1+\varepsilon_{rs})}}\right)\right\}_{th} + \left\{\left(\frac{1+\varepsilon_{\phi s}}{1+\varepsilon_{rs}}\right) * \left(\frac{1}{1+\frac{\varepsilon_{rc}-\varepsilon_{rs}}{(1+{}^{t_0}/_{c_0})(1+\varepsilon_{rs})}}\right)\right\}_{Sh}\right] \tag{5}$$

Equation (5) captures the contributions of both the thermal and shrinkage effects. Where th represents the contributions due to thermal effects and sh represents the contributions due to shrinkage effects. Equation (5) can be used to analytically predict the spring-in of angled sandwiched panels.

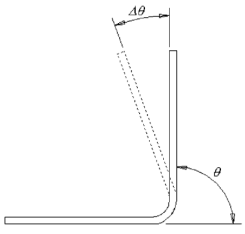

Figure 1: Angle Section showing Spring-in (Svanberg and Holmberg, 2001)

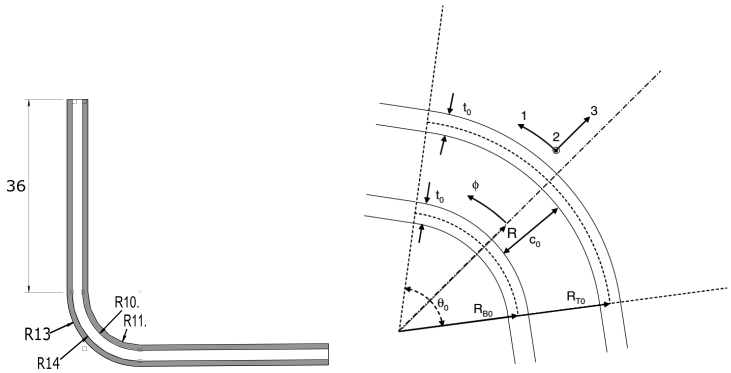

(a) Geometry (b) Dimension (Fernlund, 2005)

Figure 2: Geometry and Dimension of the Simulated Sandwich panel

Svanberg and Holmberg (2004) presented a simple mechanical constitutive model that accounted for thermal expansion, chemical shrinkage and frozen-in deformations. The model, derived in incremental form, is a limiting case of linear viscoelasticity that replaces rate dependency by path dependency. The model is applicable for a homogenized curing composite. The accuracy of the model means it can be used to study various angled structures and to predict trends.

This paper therefore aims to use the constitutive model proposed by Svanberg and Holmberg to predict the shape distortions and residual stresses present in various L-shaped Sandwich composite panels. The study is done by varying the percentage thickness of the core while keeping the overall thickness constant. Finally, the results of the simulation are compared with the results obtained via the extended analytical model.

3. FINITE ELEMENT ANALYSIS

3.1 Svanberg model

The model as described by Svanberg and Holmberg (2004) is based on incremental stresses. The constitutive equation is written as in eq. 6.

$$\Delta\boldsymbol{\sigma} = \begin{cases} \boldsymbol{C}_r\Delta(\boldsymbol{\varepsilon} - \boldsymbol{\varepsilon}_t - \boldsymbol{\varepsilon}_c) - \boldsymbol{s}, & T \geq T_g(X) \\ \\ \boldsymbol{C}_g\Delta(\boldsymbol{\varepsilon} - \boldsymbol{\varepsilon}_t - \boldsymbol{\varepsilon}_c), & T < T_g(X) \end{cases} \tag{6}$$

Where $\boldsymbol{C}_r$ is the rubbery modulus tensor and $\boldsymbol{C}_g$ is the glassy modulus tensor. In the most general situation $\Delta\boldsymbol{\sigma}$ contains six stress components: $\Delta\boldsymbol{\sigma}_{xx}$, $\Delta\boldsymbol{\sigma}_{yy}$, $\Delta\boldsymbol{\sigma}_{zz}$, $\Delta\boldsymbol{\tau}_{yz}$, $\Delta\boldsymbol{\tau}_{xz}$ and $\Delta\boldsymbol{\tau}_{yz}$.Similar observation holds for $\Delta\boldsymbol{\varepsilon}$, $\Delta\boldsymbol{\varepsilon}_t$ and $\Delta\boldsymbol{\varepsilon}_c$, each one also containing six strain components. The incremental thermal and chemical strains are computed with eq. 7 and eq. 8 respectively.

$$\Delta\boldsymbol{\varepsilon}_t = \boldsymbol{\alpha}\Delta T, \qquad \text{where} \qquad \boldsymbol{\alpha} = \begin{cases} \boldsymbol{\alpha}_l, & X < X_{gel}, T \geq T_g \\ \boldsymbol{\alpha}_r, & X \geq X_{gel}, T \geq T_g \\ \boldsymbol{\alpha}_g, & T < T_g \end{cases} \tag{7}$$

$$\Delta\boldsymbol{\varepsilon}_c = \boldsymbol{\beta}\Delta T, \qquad \text{where} \qquad \beta = \begin{cases} \boldsymbol{\beta}_l, & X < X_{gel}, T \geq T_g \\ \boldsymbol{\beta}_r, & X \geq X_{gel}, T \geq T_g \\ \boldsymbol{\beta}_g, & T < T_g \end{cases} \tag{8}$$

The state variables $\boldsymbol{s}$ also a vector can be calculated using in eq. 9

$$\boldsymbol{s}(t + \Delta t) = \begin{cases} 0, & T \geq T_g(X) \\ \\ \boldsymbol{s}(t) + (\boldsymbol{C}_g - \boldsymbol{C}_r)\Delta(\varepsilon - \varepsilon_t - \varepsilon_c), & T < T_g(X) \end{cases} \tag{9}$$

The state variables $\boldsymbol{s}$ corresponds to stresses that keep track of the loading (thermal, mechanical or shrinkage) history. In the rubbery state the state variables become zero, meaning that the stress history has been erased. In the glassy state, the s variable represent frozen-in stresses. The coefficients of thermal expansion $\boldsymbol{\alpha}$ and chemical shrinkage $\boldsymbol{\beta}$ depend on the temperature T and degree of cure X as written in eq. 7 and eq. 8 respectively. The subscripts l, r and g refer respectively to liquid, rubbery and glassy states. T_g is the glass transition temperature and X_{gel} denotes degree of cure at gelation. The glass transition temperature relates T_g to X by the DiBenedetto equation (Nielsen, 1969) stated in eq. 10. More details about the model can be obtained in Svanberg and Holmberg (2004)

$$\frac{T_g - T_{go}}{T_{g\infty} - T_{go}} = \frac{\lambda X}{1 - (1 - \lambda)X} \tag{10}$$

3.2 Model Description

The Finite Element simulation is done for a 4mm part with varying thickness of the foam core. The dimension of the L shaped part investigated is shown Fig. 2. The core thicknesses range from 12.5% thickness up to 75% while the thickness of the skin reduces correspondingly. Other details regarding the simulation can also be obtained in Makinde et al. (2017). The material coordinate system is shown in Fig. 2b. The fibre direction is the 1-direction and through the thickness direction is the 2-direction.

3.3 Material Properties

The material mechanical properties of the glass skin and the core used are in Tab. 1. For the glass-epoxy skin, the mechanical properties of fibre and matrix laminate (glassy and rubbery state) were calculated using self-consistent-field micro-mechanics obtained from Bogetti et al. (1995) and 3D-laminate theory obtained from Chen and Tsai (1996). Mechanical properties of E-glass fibres were found in Kaw (2005) while the properties of the matrix was obtained from Svanberg and Holmberg (2001). The fibre Volume fraction used was 49%. The models used to predict laminate properties does not account for the waviness of fibreglass weave. For the core, the mechanical properties were obtained from Fernlund (2005). The core remains stable even at high temperatures hence there is no rubbery phase or liquid phase in the properties of the core. For the composite skin, the mechanical properties in the liquid phase is assumed to be zero while X_{gel} occurs at 34%.

Table 1: Mechanical Properties of Glass-Epoxy skin (V_f = 49 $\%$) and Di-vinyl Cell Foam Core

Property	**Value**		**Di-vinyl Core**	**Units**
	Rubbery	**Glassy**		
E_{11} = E_{22}	22.9	18.69	138	Gpa
E_{33}	8.48	2.31	138	Gpa
ν_{12}	0.09	0.0021	0.32	-
ν_{13} =ν_{23}	0.45	0.85	0.32	-
G_{12}	2.55	2.75e-02	33	Gpa
G_{13} = G_{23}	2.43	2.74e-02	33	Gpa
α_{11} = α_{22}	15.15	5.49	3.5e-5	$10e^{-6}/°C$
α_{33}	6.65	264.8	3.5e-5	$10e^{-6}/°C$
β_{11} = β_{22}	-3.6e-03	-7.91e-05	0	$10e^{-6}/°C$
β_{33}	-0.022	-0.0351	0	$10e^{-6}/°C$

3.4 Meshing and Boundary Conditions

The mesh and boundary conditions for the L shaped section is shown in Fig. 3. A total of 8 elements are used in the through-the-thickness direction. Also Fig. 3 shows the principal coordinates of the part . The constitutive model has been implemented in ABAQUS as a user subroutine, UMAT by using a 4-node bilinear plane strain quadrilateral element with reduced integration and hourglass control (CPE4R) (Manual, 2010). For the boundary conditions, the whole model was done in 2 steps. In the first step, which models the in mould phase of the manufacturing, the whole part was fully constrained. In the second step which modelled the demoulded part, the boundary condition was to restrict rigid body motion. The boundary condition to restrict rigid body motion include

- Point A in Fig. 3 was fully constrained therefore $U_1 = U_2 = 0$.
- Point B in Fig. 3 was constrained in the y-direction therefore $U_2 = 0$.

- Only half of the L-section is modelled, taking advantage of the symmetry along line C.

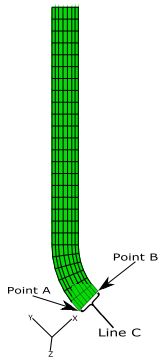

Figure 3: Angle Section showing Spring-in (Svanberg and Holmberg, 2001)

4. RESULTS AND DISCUSSION

4.1 Analytical Results

Table 2 shows the results obtained using Eq. 5. the values obtained in column 2 are based on plane strain assumptions. Also it is assumed that $\varepsilon_1 = \varepsilon_2 = 0$. This means that the skin and the core do not deform in the in plane directions. Column 3 is calculated based on Eq.17a in Fernlund (2005). For columns 5 and 6, The values of the cure shrinkage coefficient was used. Since the core is not expected to undergo shrinkage, then the value is zero. From column 4, it can be seen that the core has an increasing effect on the thermal behaviour of the part. As the percentage of the part increases, the contribution of the core towards the overall thermal spring-in increases. In the case of column 7, the increase in the percentage of the core, reduces the spring-in of the part. Overall, the increase in the percentage volume of the core brings about the reduction in the spring-in angle.

Table 2: Analytical Results obtained from Eq. 5

Description	Thermal			Chemical Shrinkage			**Total Spring-in** (^{o})
	$\varepsilon_{\phi s}$	ε_R	Spring-In(^{o})	$\varepsilon_{\phi s}$	ε_R	Spring-In(^{o})	
$0\%^a$	0	-8.17E-3	0.74	-3.6E-3	-2.2E-2	1.69	2.43
$12.5\%^b$	0	-6.79E-3	0.71	0	0	1.25	1.96
$25\%^b$	0	-6.79E-3	0.69	0	0	0.89	1.58
$37.5\%^b$	0	-6.79E-3	0.67	0	0	0.61	1.28
$50\%^b$	0	-6.79E-3	0.66	0	0	0.37	1.03
$62.5\%^b$	0	-6.79E-3	0.64	0	0	0.17	0.81
$75\%^b$	0	-6.79E-3	0.63	0	0	-0.01	0.63

^{a} skin without core
^{b} skin without percentage Core

4.2 Finite Element Analysis Results

Figure 4 shows the stress deformation of the simulations. Fig. 4(a) is the stress plot of the part with no core while Fig. 4(b) is the stress plot of the part with 25% core. Fig. 4(c) is the stress plot of the part with 50% core while Fig. 4(d) is the stress plot of the part with 75% core.

Figure 5 shows the displacement results of the analysis. Fig. 5(a) is the displacement plot of the part with no core while Fig. 5(b) is the displacement plot of the part with 25% core. Fig. 5(c) is the displacement plot of the part with 50% core and Fig. 5(d) is the displacement plot of the part with 75% core.

From the plotted results in Fig. 4 and Fig. 5, it is seen that the stresses in the part increases as the core thickness increases. The increase in the stresses in the part is associated with the increase in the bending resistance of the whole part due to the increase of the core. This factor also contributes to the reduction in the deformation of the part as the core thickness increases.

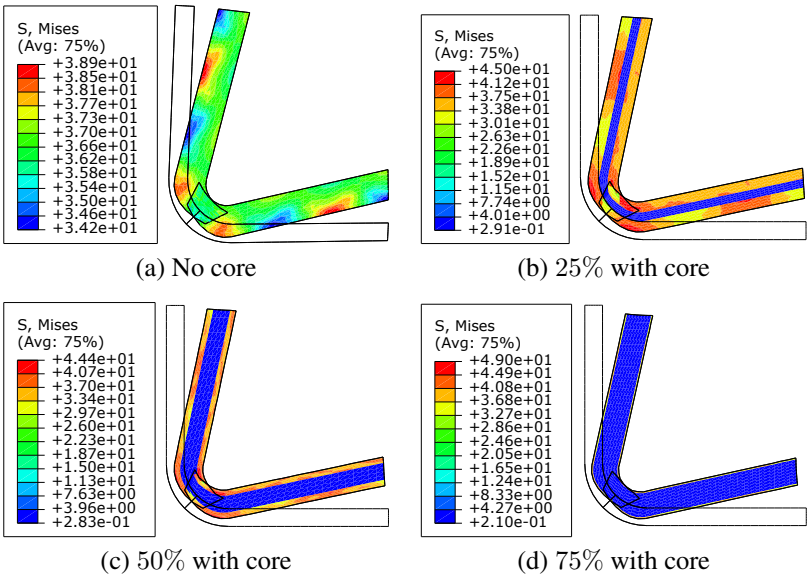

(a) No core (b) 25% with core

(c) 50% with core (d) 75% with core

Figure 4: Stress deformation of the sandwich panels with varying percentages of the core

4.3 Comparison of Results

Figure 6 shows the spring-in predictions of the analytical model in comparison to Svanberg model implemented in Abaqus. The results shows the spring-in predictions for both the Analytical and Svanberg model. The figure highlights the various contributions of the cure shrinkage and the thermal effects. It shows that relatively, the percentage contribution of the thermal effect gradually increases in value as shrinkage property gradually reduces. The figure also shows that the shrinkage effect has the most influential contribution to the spring-in phenomenon while the thermal effect is relatively constant. Furthermore, a comparison of the analytical model and the Svanberg model shows that the analytical model over estimates spring-in values than that of the Svanberg model.

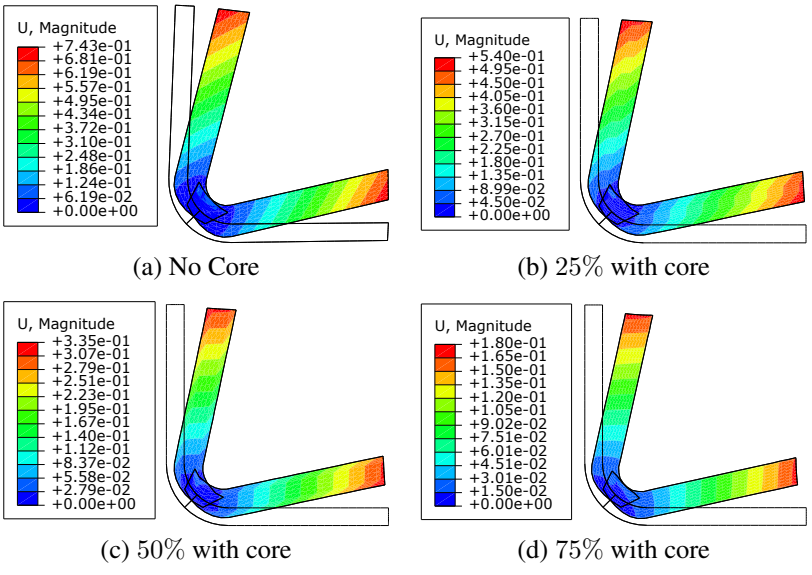

(a) No Core (b) 25% with core

(c) 50% with core (d) 75% with core

Figure 5: Displacement of the sandwich panels with varying thicknesses of the core

4.3.1 Comparison of UD fibres with Woven fibres

A comparison of the results of the UD fibres against the woven fibre results show that the thermal contributions to the spring-in effect were quite equal while the contributions of the shrinkage effect differed considerably. As the percentage

of the core increased, the shrinkage effect contribution to the overall spring-in reduces. This causes the spring-in of the woven fibres to reduce considerably even lower than the UD fibres.

4.3.2 Comparison of Glass materials with Carbon materials

A comparison of the glass and carbon results shows that the UD glass fibre thermal contribution to spring-in exceeded that of the UD carbon. Also, the shrinkage contribution of the UD glass was equally higher than that of the UD carbon. This means that UD Glass sandwich panels would generally experience more spring-in than the UD Carbon. Additionally, the thermal contribution of the glass woven fibre is higher than that of woven carbon while the shrinkage contribution of the woven carbon fibre is higher than that of the glass. Overall, the woven carbon fibre has higher spring-in as the core increases.

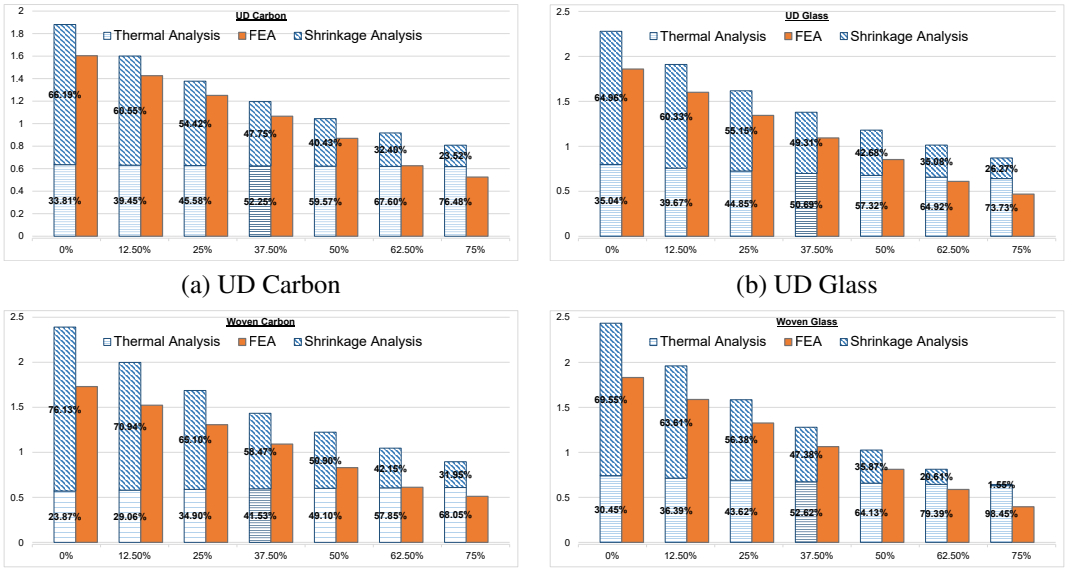

(a) UD Carbon (b) UD Glass

(c) Woven Carbon (d) Woven Glass

Figure 6: Spring-in Predictions for Analytical model and FEA

5. CONCLUSION

Sandwich constructions are used in the Aerospace and wind turbine industry, due to their high stiffness to weight ratio and their high resistance to bending . However, angled sandwich panels experience spring-in effect and the resulting problem is often greater than those experienced by solid laminates due to their inherent strengths. The core influences the thermal response of the structure while also contributing to reducing the deformation of the part due to cure shrinkage.

In this paper, the analytical model developed by Fernlund for sandwich was extended to capture cure shrinkage effect. The results of the extended model enables the evaluation of the contributions of each effect (thermal and cure shrinkage) to the overall spring-in phenomenon even with varying percentage contribution from the core and skin. The evaluation of the analytical results shows that the thermal contribution of the sandwich panels remain fairly constant irrespective of the percentage content of the sandwich core while the contributions of the shrinkage effect reduces.

In addition, Svanberg's model was used to simulate various percentages of sandwich core in an angled sandwich panel. The results shows that with the increasing percentage of the sandwich core, the spring-in angle reduces while there is a corresponding increase in the amount of residual stresses in the part.

Finally, the results of the analytical model was then compared with Svanberg model implemented using UMAT in Abaqus. The results of both models show good accuracy in their prediction of Spring-in behaviours of Composite Sandwich panels. Comparison of the results show that the extended analytical model over predicts the spring-in phenomenon in all cases. Furthermore, it shows that the shrinkage contribution to the spring-in effect is the most influential to the overall phenomenon. The study could be replicated for other sandwich structures like Top hat stiffeners, U shaped and Z shaped structures.

6. ACKNOWLEDGEMENTS

This work was performed in Instituto Tecnologico de Aeronatica, Brazil, and was funded by the Nigerian Air Force and CNPq (grants 300886/2013-6 and 301053/2016-2)

7. REFERENCES

Travis A Bogetti, Christopher P Hoppel, and William H Drysdale. Three-dimensional effective property and strength prediction of thick laminated composite media. Technical report, DTIC Document, 1995.

Hong-Ji Chen and Stephen W Tsai. Three-dimensional effective moduli of symmetric laminates. *Journal of Composite Materials*, 30(8):906–917, 1996.

Alfredo Faria. Prediction of post cure residual stresses and distortions in the fabrication of composite structures, 2015.

Göran Fernlund. Spring-in of angled sandwich panels. *Composites science and technology*, 65(2):317–323, 2005.

Andrew Johnston, Pascal Hubert, Göran Fernlund, Reza Vaziri, and Anoush Poursartip. Process modeling of composite structures employing a virtual autoclave concept. *Science and Engineering of Composite Materials*, 5(3-4):235–252, 1996.

Autar K Kaw. *Mechanics of composite materials*. CRC press, 2005.

Yeong K Kim and Scott R White. Viscoelastic analysis of processing-induced residual stresses in thick composite laminates. *Mechanics Of Composite Materials And Structures An International Journal*, 4(4):361–387, 1997.

Yusuf Mahadik and K Potter. Experimental investigation into the thermoelastic spring-in of curved sandwich panels. *Composites Part A: Applied Science and Manufacturing*, 49:68–80, 2013.

OM Makinde, AR Faria, and MV Donadon. Prediction of shape distortions in angled composite structures. In *Proc. 6th Int. Symposium on Solid Mechanics*, page 302, 2017.

Abaqus Users Manual. Version 6.10. *ABAQUS Inc*, 2010.

Lawrence E Nielsen. Cross-linking–effect on physical properties of polymers. 1969.

S Pagliuso. Warpage, a nightmare for composite parts producers. *Progress in science and engineering of composites*, 1617, 1982.

DW Radford and TS Rennick. Determination of manufacturing distortion in laminated composite. In *Proc. 11th Int. Conf. Compos. Mater. Compos. Process.: Microstruct Woodhead Publishing*, page 302, 1997.

Christopher Ridgard. Accuracy and distortion of composite parts and tools: causes and solutions. *TECHNICAL PAPERS-SOCIETY OF MANUFACTURING ENGINEERS-ALL SERIES-*, 1993.

A Stephan, E Schwinge, J Muller, and H Ory. On the springback effect of cfrp stringers: an experimental, analytical and numerical analysis. In *INTERNATIONAL SAMPE TECHNICAL CONFERENCE*, volume 28, pages 245–254, 1996.

J Magnus Svanberg and J Anders Holmberg. Prediction of shape distortions part i. fe-implementation of a path dependent constitutive model. *Composites part A: applied science and manufacturing*, 35(6):711–721, 2004.

JM Svanberg and JA Holmberg. An experimental investigation on mechanisms for manufacturing induced shape distortions in homogeneous and balanced laminates. *Composites Part A: Applied Science and Manufacturing*, 32(6): 827–838, 2001.

T-M Wang, IM Daniel, and JT Gotro. Thermoviscoelastic analysis of residual stresses and warpage in composite laminates. *Journal of Composite Materials*, 26(6):883–899, 1992.

H.W. Wiersma, L.J.B. Peeters, and R. Akkerman. Prediction of springforward in continuous-fibre/polymer l-shaped parts. *Composites Part A: Applied Science and Manufacturing*, 29(11):1333 – 1342, 1998a.

HW Wiersma, LJB Peeters, and R Akkerman. Prediction of springforward in continuous-fibre/polymer l-shaped parts. *Composites Part A: Applied Science and Manufacturing*, 29(11):1333–1342, 1998b.

8. RESPONSIBILITY NOTICE

The authors are the only responsible for the printed material included in this paper